

Disasters with relation to rock mechanics

Author: Prof. Dr. habil. Heinz Konietzky
(TU Bergakademie Freiberg, Geotechnical Institute)

- 1 Introduction..... 2
- 2 Seismicity 4
- 3 Sinkholes..... 9
- 4 Mass movements 13
- 5 Explosions..... 23
- 6 References 25

1 Introduction

This chapter discusses disasters with direct link to geomechanics. Most essential phenomena, their causes and implications are presented. Disasters can be categorised as follows:

- based on origin:
 - man-made disasters
 - natural disasters
- based on type of movement
 - falls
 - topples
 - slides
 - flows
- based on material involved:
 - soil
 - rock
 - debris
 - snow

Natural disasters comprise mainly:

- Earthquakes
- Floods
- Mass movements (avalanches, rockfall, debris flow etc.)
- Sinkholes caused by natural processes

Man-made disasters comprise mainly:

- Induced seismicity (mining induced, geothermal induced etc.)
- Sinkholes caused by man-made activities (old mining etc.)
- Explosions, e.g. nuclear explosions

In respect to disasters geo-engineers have to consider the following tasks:

- Prediction of disasters (e.g. probability of failure, prediction in space and/or time)
- Prediction of potential impacts (consequences)
- Risk analysis (product of probability of failure and cost of failure)
- Design of countermeasures (e.g. protective barriers, reinforcements etc.)
- Monitoring of disaster prone sites (e.g. geodetic measurements, seismic monitoring etc.)
- Backanalysis of disasters (investigation of causes)

Risk analysis has to consider acceptable risks. Often risk is referred to fatalities per time. Public risk is often assumed to be in the order of $1 \cdot 10^{-4}$ /year (Fenton & Griffiths, 2008). This can be compared with human caused or natural disasters, e.g.:

- accident death rate: $1 \cdot 10^{-4}$ /year
- accident deaths from electric current: $5 \cdot 10^{-6}$ /year
- fire accident death rate: $4 \cdot 10^{-5}$ /year
- accidental deaths from lightning, tornados, hurricans: $1 \cdot 10^{-6}$ /year

As Fig. 1 documents, earthquakes and associated tsunamis, floods and landslides are the most dangerous and costlies events worldwide.

Loss events worldwide 1980 – 2015
10 costliest events ordered by overall losses

Date	Event	Affected area	Overall losses in US\$ m original values	Insured losses in US\$ m original values	Fatalities
11.3.2011	Earthquake, tsunami	Japan: Aomori, Chiba, Fukushima, Ibaraki, Iwate, Miyagi, Tochigi, Tokyo, Yamagata	210,000	40,000	15,880
25-30.8.2005	Hurricane Katrina, storm surge	United States: LA, MS, AL, FL	125,000	60,500	1,720
17.1.1995	Earthquake	Japan: Hyogo, Kobe, Osaka, Kyoto	100,000	3,000	6,430
12.5.2008	Earthquake	China: Sichuan, Mianyang, Beichuan, Wenchuan, Shifang, Chengdu, Guangyuan, Ngawa, Ya'an	85,000	300	84,000
23-31.10.2012	Hurricane Sandy, storm surge	Bahamas, Cuba, Dominican Republic, Haiti, Jamaica, Puerto Rico, United States, Canada	68,500	29,500	210
17.1.1994	Earthquake	United States: Northridge, Los Angeles, San Fernando Valley, Ventura	44,000	15,300	61
1.8-15.11.2011	Floods, landslides	Thailand: Phichit, Nakhon Sawan, Phra Nakhon Si Ayuttaya, Phthumthani, Nonthaburi, Bangkok	43,000	16,000	813
6-14.9.2008	Hurricane Ike	United States, Cuba, Haiti, Dominican Republic, Turks and Caicos Islands, Bahamas	38,000	18,500	170
27.2.2010	Earthquake, tsunami	Chile: Concepción, Metropolitana, Rancagua, Talca, Temuco, Valparaiso	30,000	8,000	520
23./24./27.10.2004	Earthquake	Japan: Honshu, Niigata, Ojiya, Tokyo, Nagaoka, Yamakoshi	28,000	760	46

Source: Munich Re, NatCatSERVICE, 2016

© 2016 Münchener Rückversicherungs-Gesellschaft, Geo Risks Research, NatCatSERVICE As at: March 2016

Fig. 1: Costliest natural events between 1980 and 2015 (Munich Re, 2016)

2 Seismicity

Natural seismicity is mainly caused by:

- Plate tectonics
- Vulcano activities

The following types of induced seismicity can be distinguished:

- Mining-induced seismicity (e.g. underground mining, storage in cavern)
- Injection-induced seismicity (e.g. deep geothermal projects, injection of fluids into porous or fractures rocks, fracking)
- Explosion or blasting induced vibrations (e.g. nuclear explosions, mine and tunnel blasting)
- Water reservoir induced seismicity (e.g. change in water level)

Problems with induced seismicity are observed world-wide, especially in relation to:

- Mining (especially salt and potash mining, coal mining, but also ore mining at great depths) and
- Deep geothermal energy projects.

Strongest natural earthquakes have reached a magnitude of 9 or even slightly above. They are mainly located along the plate boundaries as shown in Fig. 2. The strongest mining induced events reached magnitudes of about 5 in mining, 3 for deep geothermal projects, 3.5 for water reservoirs and 4 in petroleum engineering (see also Fig. 3 and 4).

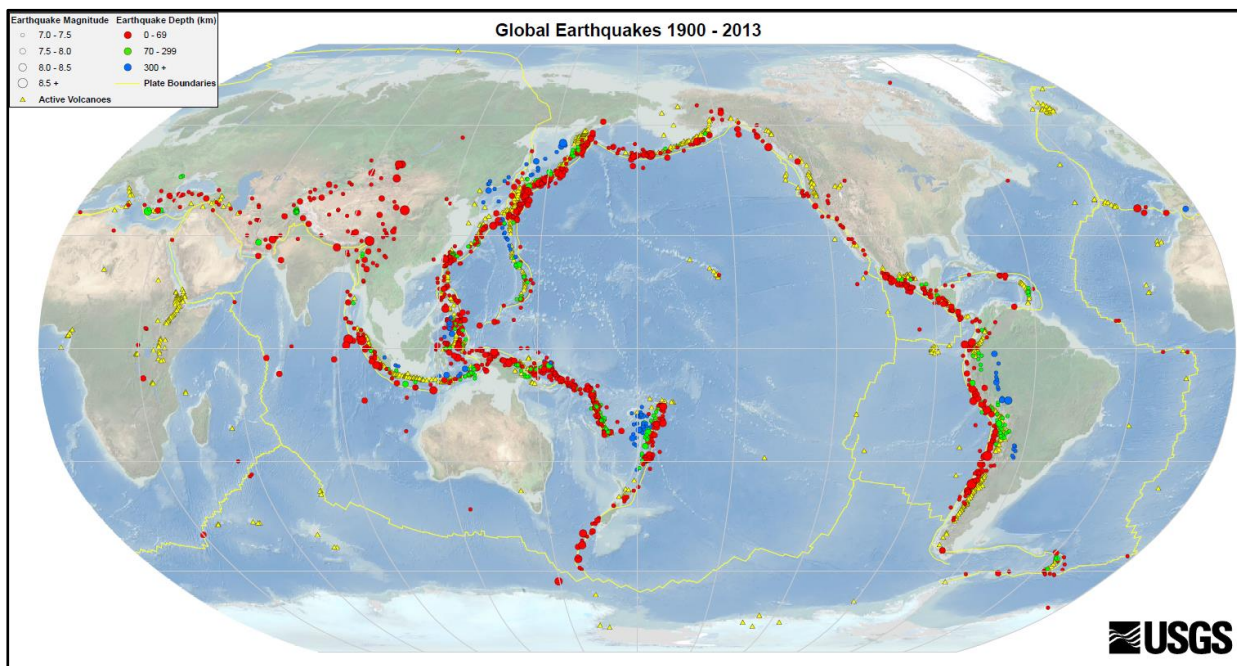


Fig. 2: Seismicity of the earth (data from 1900 to 2013, USGS)

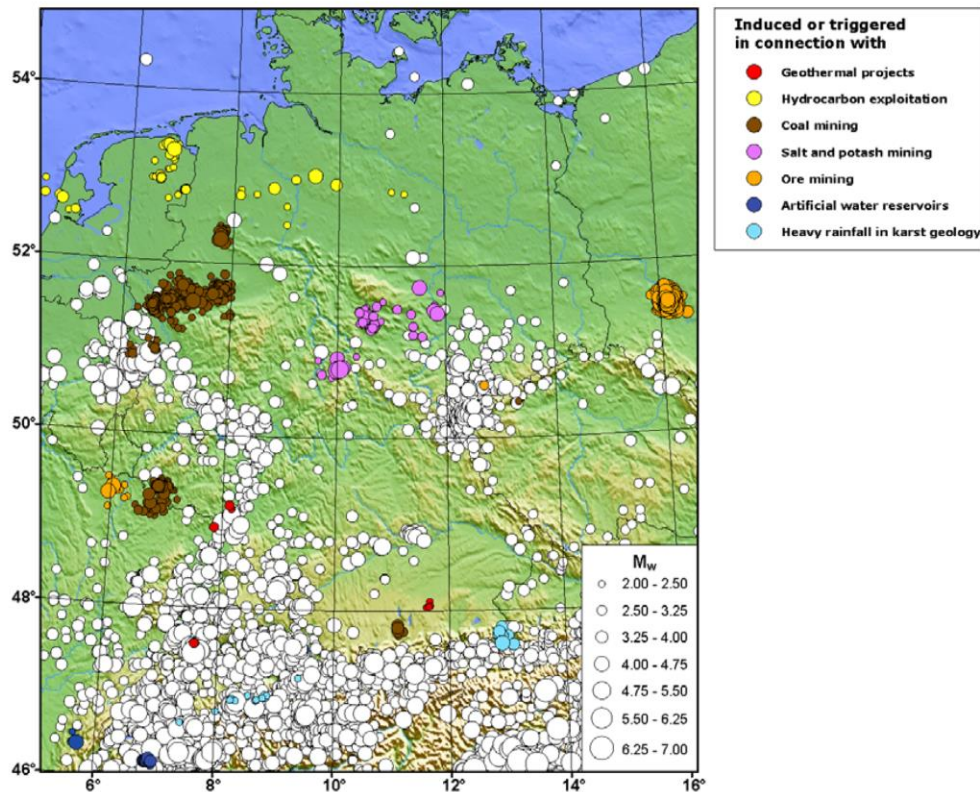


Fig. 3. Overview about natural and induced seismicity in Germany and neighbouring countries (Grünthal, 2014)

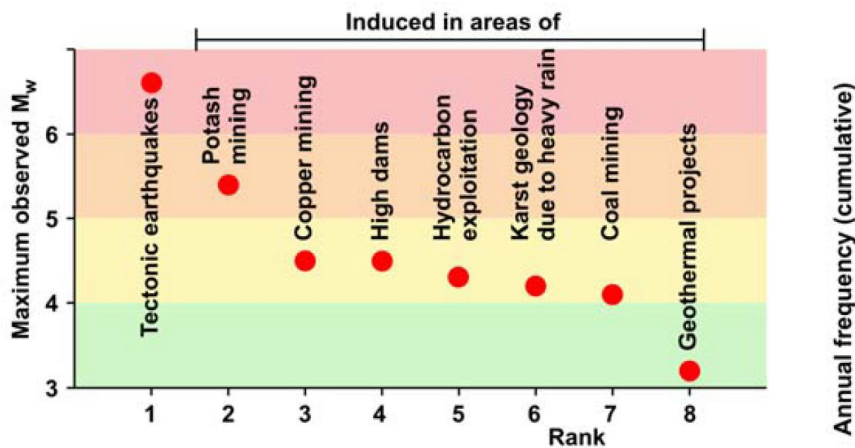


Fig. 4. Overview of observed maximum magnitudes in Europe (Grünthal, 2014)

Damage produced by seismicity can be quite diverse:

- Damage of buildings and infrastructural elements by shaking, especially by surface waves
- Damage by seismic triggered mass movements (landslides, rockfall etc.)
- Seismic induced tsunamis and floodings
- Environmental pollution (nuclear power plant damage, waste water dam breakage etc.)

In engineering seismology most often vibration velocity is used as a measure to quantify vibrations or tremors (see also Fig. 5). Different regulations set limits for maximal vibration velocities (Fig. 6 and Tab. 1). These values usually define categories due to construction stability or utilization purpose. The critical values are also frequency dependent as wave energy is frequency depending.

Based on numerical simulations **Peak Ground Velocity (PGV)** can be predicted for induced or natural earthquakes based on site-specific data. Exemplary, Fig. 7 and 8 show results for predicted PGV for mine flooding induced seismic events. If enough seismological data are available, the so-called Gutenberg-Richter-Relation (Fig. 9) can be established to predict the maximum expectable magnitude: in this specific case about -0.5 for locations inside the schist and about 2.3 for the granitic formation.

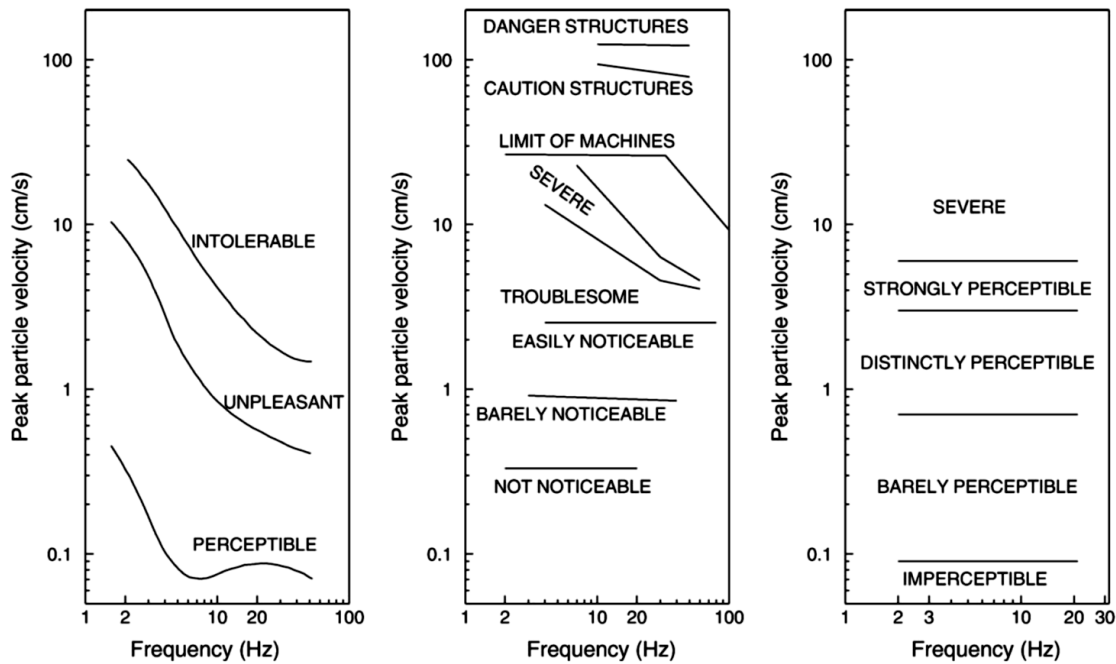


Fig. 5: Vibration levels, left: recommended, middle: traffic related, right: thresholds for pile driving (Bommer et al. 2006)

Tab. 1: Limit values for vibration velocities (DIN 4150-3). 100 Hz – values are used for for higher frequencies.

building type	Peak Particle Velocities (Vibration Velocities) (mm/s)			
	basement frequencies			uppermost top slab, horizontal all frequencies
	1 Hz to 10 Hz	10 Hz to 50 Hz	50 Hz to 100 Hz	
industrial used buildings	20	20 to 40	40 to 50	40
residential buildings	5	5 to 15	15 to 20	15
Highly sensitive buildings (e.g. historical monuments)	3	3 to 8	8 to 10	8

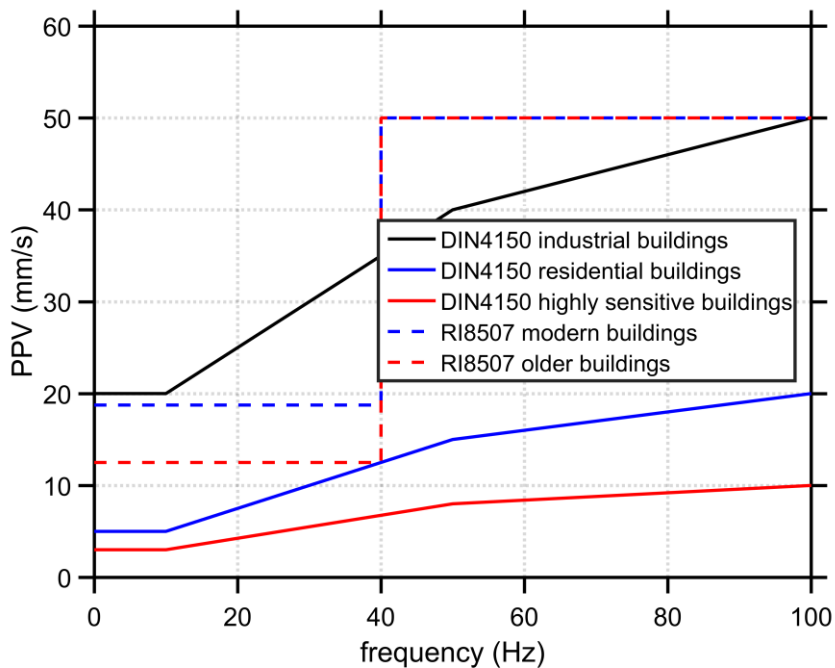


Fig. 6: Frequency dependent limit values for vibration velocities, comparing German Standard DIN4150-3 (DIN4150) and USBM recommendations RI8507 (Siskind et al. 1980).

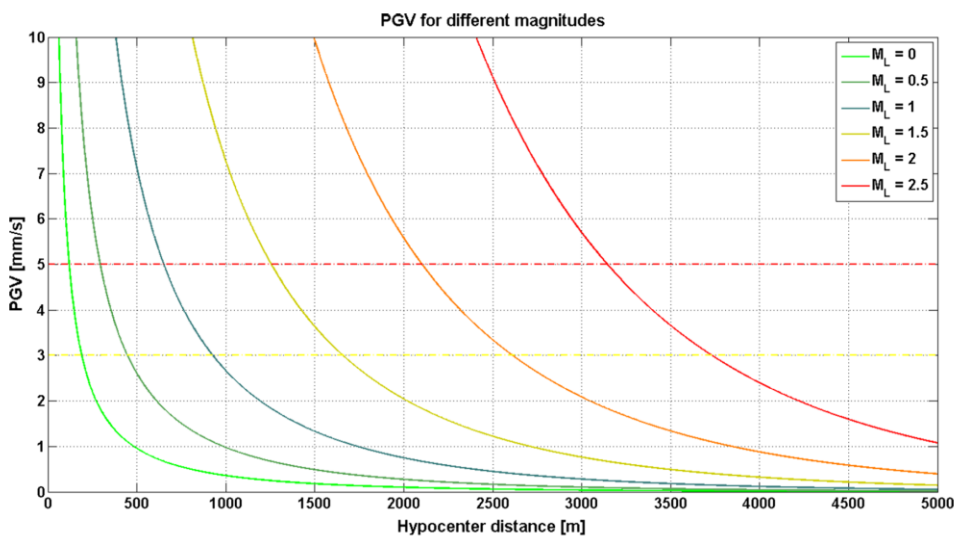


Fig. 7: Site-specific prediction of PGV as function of hypocenter distance and local magnitude (Schütz & Konietzky 2016)

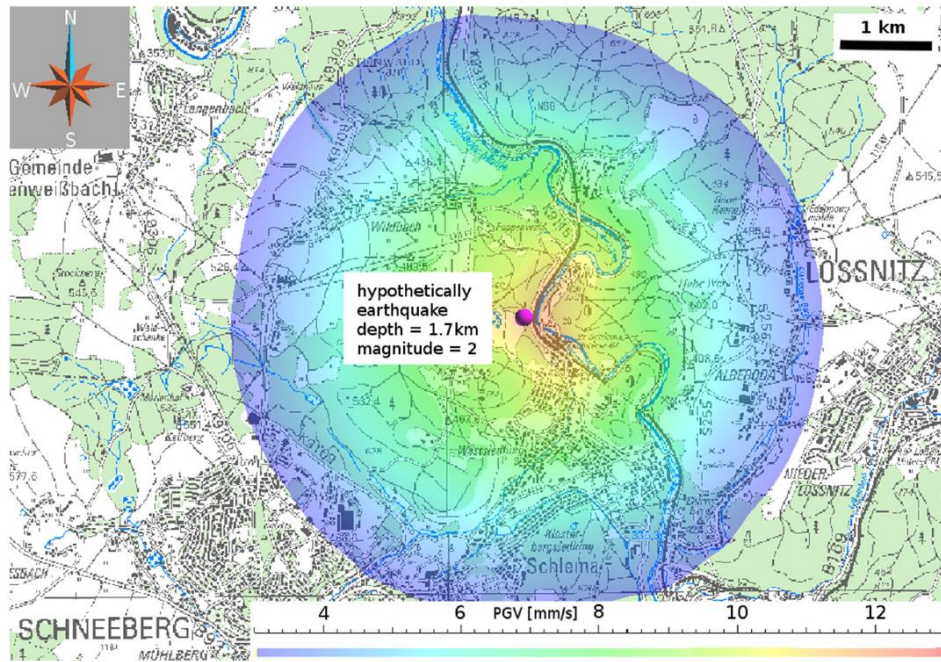


Fig. 8: Site-specific prediction of PGV distribution at the surface for an induced event with magnitude 2 at a depth of 2 km (Schütz & Konietzky 2016)

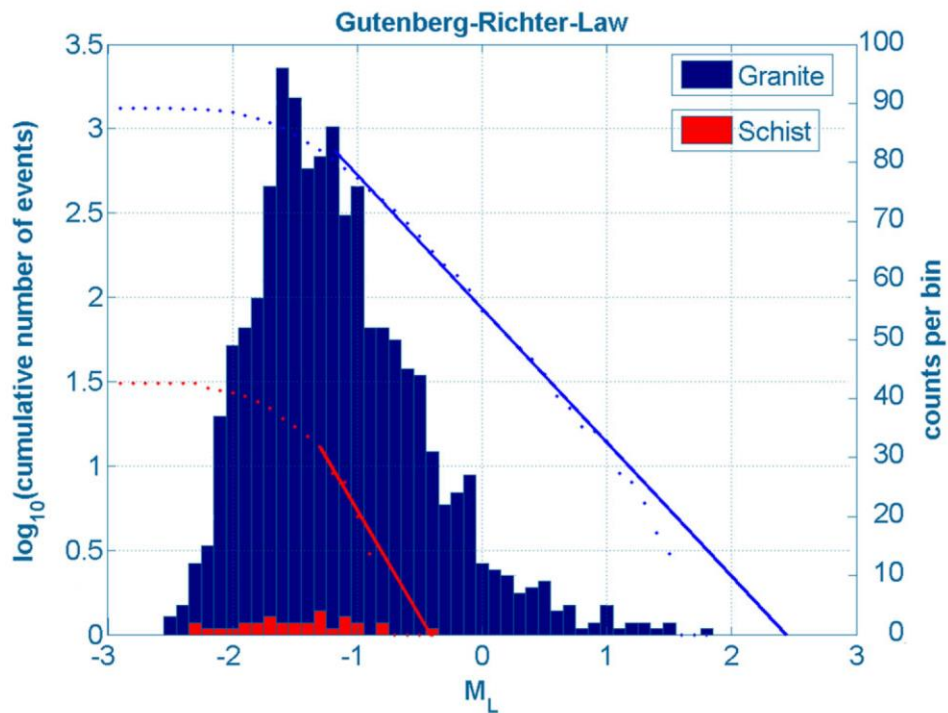


Fig. 9: Gutenberg-Richter-Relation for induced seismic events in granite and schist formation (Schütz & Konietzky 2016)

3 Sinkholes

Sinkholes can be formed by natural underground processes like solution of highly soluble rocks (e.g. carbonatic rocks like limestone, anhydrite or gypsum) or suffosion (water driven removal of small particles producing local mass deficits). In both cases large underground cavities are created over a long period of time. These cavities are growing until they reach a critical size followed by sudden collapses. Besides natural processes sinkholes can also be created by human activities, like mining, tunneling, operation of caverns or leakage of underground water pipes. Exemplary, Figs 10 to 14 show some spectacular sinkholes. Figs 15 to 17 give some impression of one of the biggest natural sinkholes world-wide situated in China, Dabaschan region, called 'Xiaozhai pit' (limestone): 600 m deep and diameter of 500 m comprising 1.2 billion m³. This sinkhole is connected to a 20 km long underground river system.



Fig. 10: Sinkhole (created by near surface tunneling, Japan, 2016)



Fig. 11. Sinkhole (created by flooding and pipe leakage, Guatemala, 2010)



Fig. 12: Sinkhole (created by solution of a salt dome, Germany, 2010)



Fig. 13: Sinkhole (created by underground copper mining, Kazakhstan, 2009)



Fig. 14: Sinkhole (created by natural solution process, Germany, 2010)

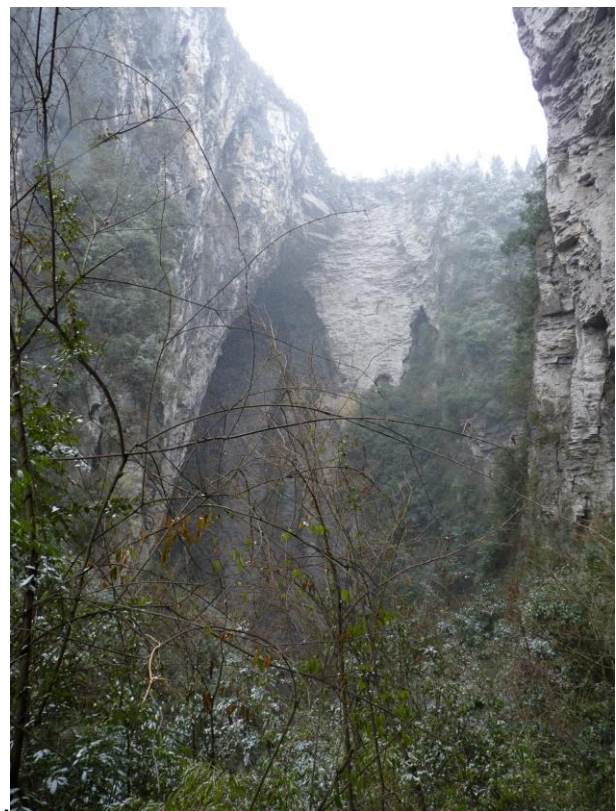


Fig. 15: 'Xiaozhai pit' sinkhole, China.



Fig. 16: 'Xiaozhai pit' sinkhole, China



Fig. 17: 'Xiaozhai pit' sinkhole, China

4 Mass movements

Mass movements are mainly driven by gravity or ground movements. Several events like earthquakes, floods or heavy rainfall can trigger such mass movements. The term mass movement covers bulk movements of soil and rock debris and can also include snow avalanches. These processes can be quite fast (up to 100 km/h or faster), but also very slow (creep phenomena).

Although it is still hardly possible to predict mass movements in time - location, run-out and risk can be estimated. Depending on type of mass movement and required quality different calculation methods are available:

- Continuum based mechanical and hydro-mechanical coupled approaches (FEM, FDM)
- Discontinuum based mechanical and hydro-mechanical coupled approaches (SPH, DEM, DDA, Particle Methods)
- Continuum fluid mechanical approaches (CFD)
- Key block analysis
- Probabilistic rockfall simulation tools based on rolling, falling and jumping balls (rockfall trajectory analysis)
- Run-out prediction tools based on different physical approaches

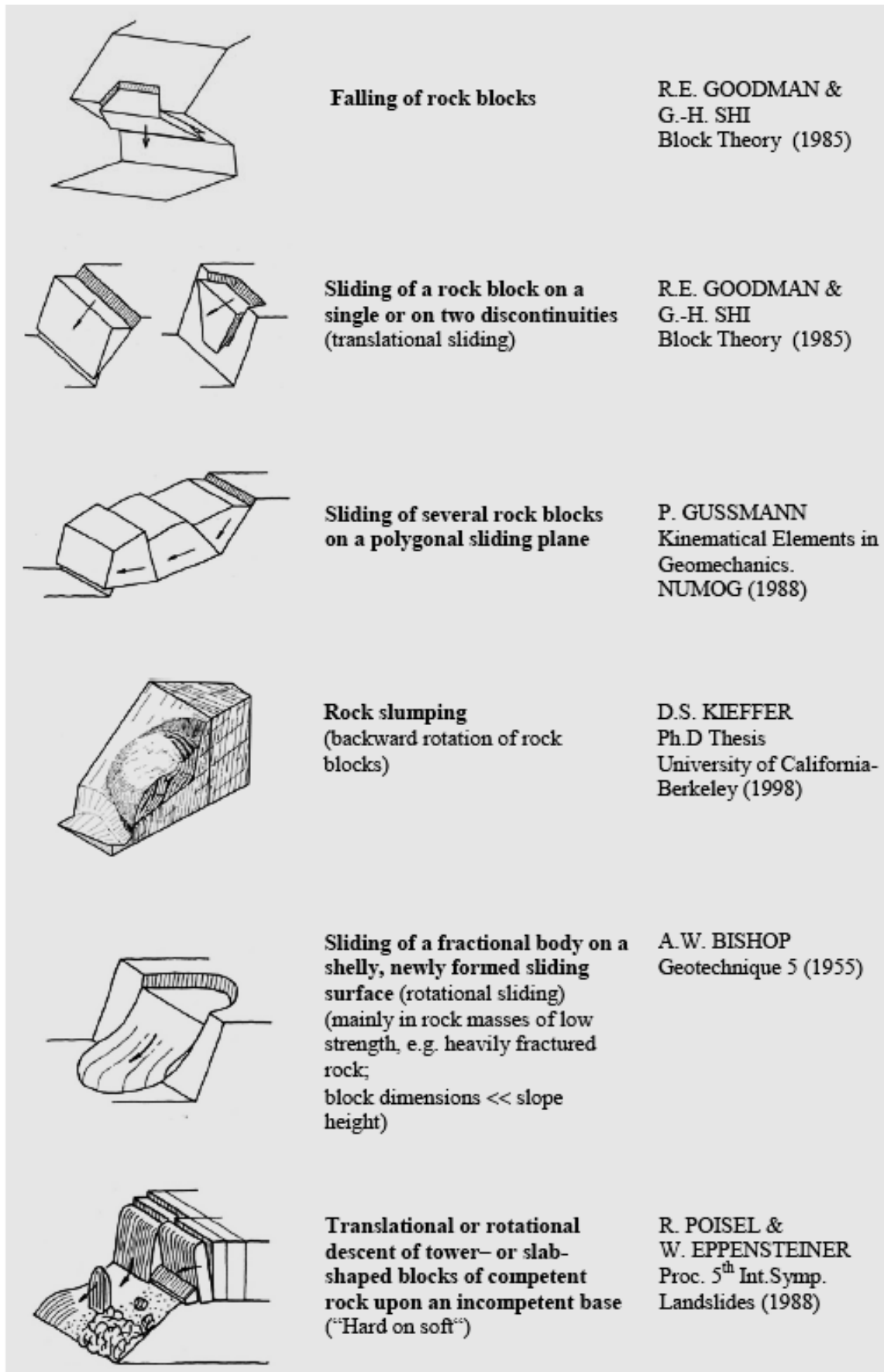
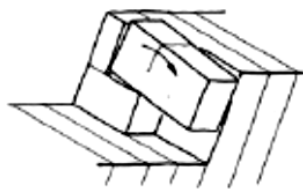


Fig. 18 (part 1): Classification of mass movements (Poisel & Preh, 2004)



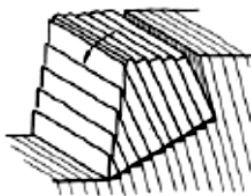
Rotation of single rock blocks
(e. g. rotation of a rock block on a discontinuity due to eccentric bearing or partial yielding of bearing, slumping of one single rock block)

W. WITTKE
Rock Mechanics.
Springer (1990)



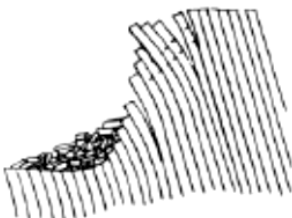
Buckling of column- or slab-shaped rock blocks
(column- or slab thickness \ll slope height)

D. S. CAVERS
Rock Mechanics 14
(1981)



Toppling of column- or slab-shaped rock blocks
(forward rotation similar to dominos; mainly when joint strength is low and rock block strength is high)

R.E GOODMAN &
J.W. BRAY
Proc. Conf. Rock Eng.
for Foundations
and Slopes (1976)



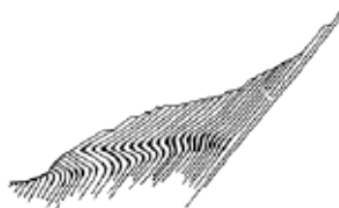
Flexural toppling
bending of column- or slab shaped rock blocks like cantilever beams

M. HITTINGER &
R.E GOODMAN
Report, University of
California, Berkeley
(1978)



Slope creep
Continuously decreasing creep of rock mass downslope with increasing depth
(mainly in rock masses of low strength, e.g. shales, phyllites)

O.C. ZIENKIEWICZ,
C. HUMPHESON &
R.W. LEWIS
Geotechnique 25 (1975)



Kink band slumping
S-shaped deformation of rock lamellae due to slope creep

A. PREH
PhD Dissertation,
Vienna University of
Technology (2004)

Fig. 18 (part 1): Classification of mass movements (Poisel & Preh, 2004)

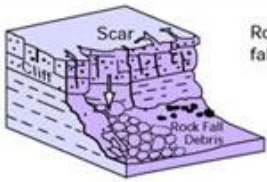
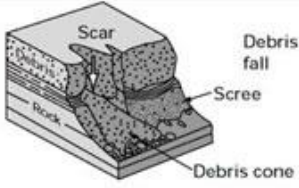
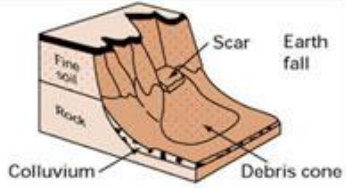
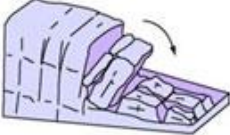

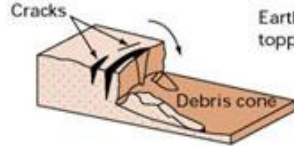
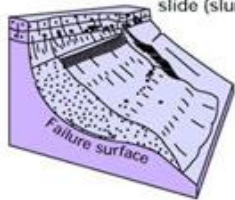
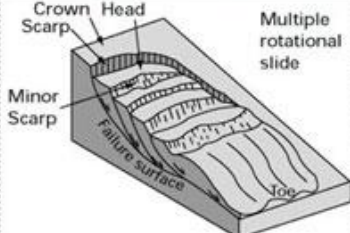
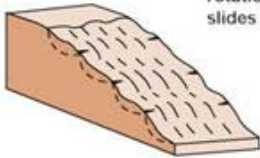
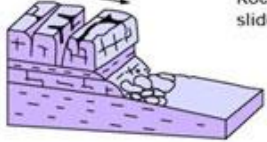
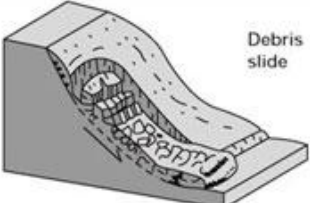
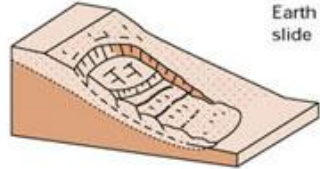
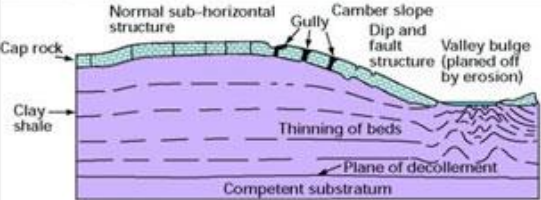

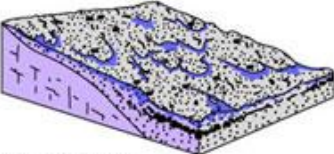
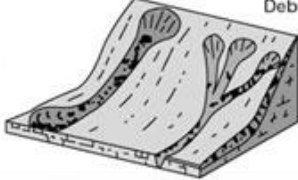


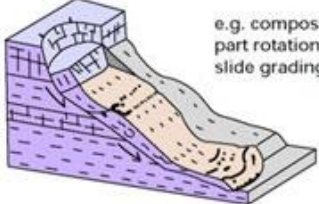
Material		ROCK	DEBRIS	EARTH
Movement type				
FALLS		 <p>Rock fall</p>	 <p>Debris fall Scree Debris cone</p>	 <p>Earth fall Scar Colluvium Debris cone</p>
		 <p>Rock topple</p>	 <p>Debris topple Debris cone</p>	 <p>Earth topple Cracks Debris cone</p>
SLIDES	Rotational	 <p>Single rotational slide (slump) Failure surface</p>	 <p>Multiple rotational slide Crown Scarp Head Scarp Minor Scarp Failure surface Toe</p>	 <p>Successive rotational slides</p>
	Translational (Planar)	 <p>Rock slide</p>	 <p>Debris slide</p>	 <p>Earth slide</p>
SPREADS	 <p>e.g. cambering and valley bulging</p>			 <p>Earth spread</p>
FLOWS	 <p>Solifluction flows (Periglacial debris flows)</p>	 <p>Debris flow</p>	 <p>Earth flow (mud flow)</p>	
COMPLEX	 <p>e.g. Slump-earthflow with rockfall debris</p>		 <p>e.g. composite, non-circular part rotational/part translational slide grading to earthflow at toe</p>	

Fig. 19: Classification of mass movements (BGS, 2016)

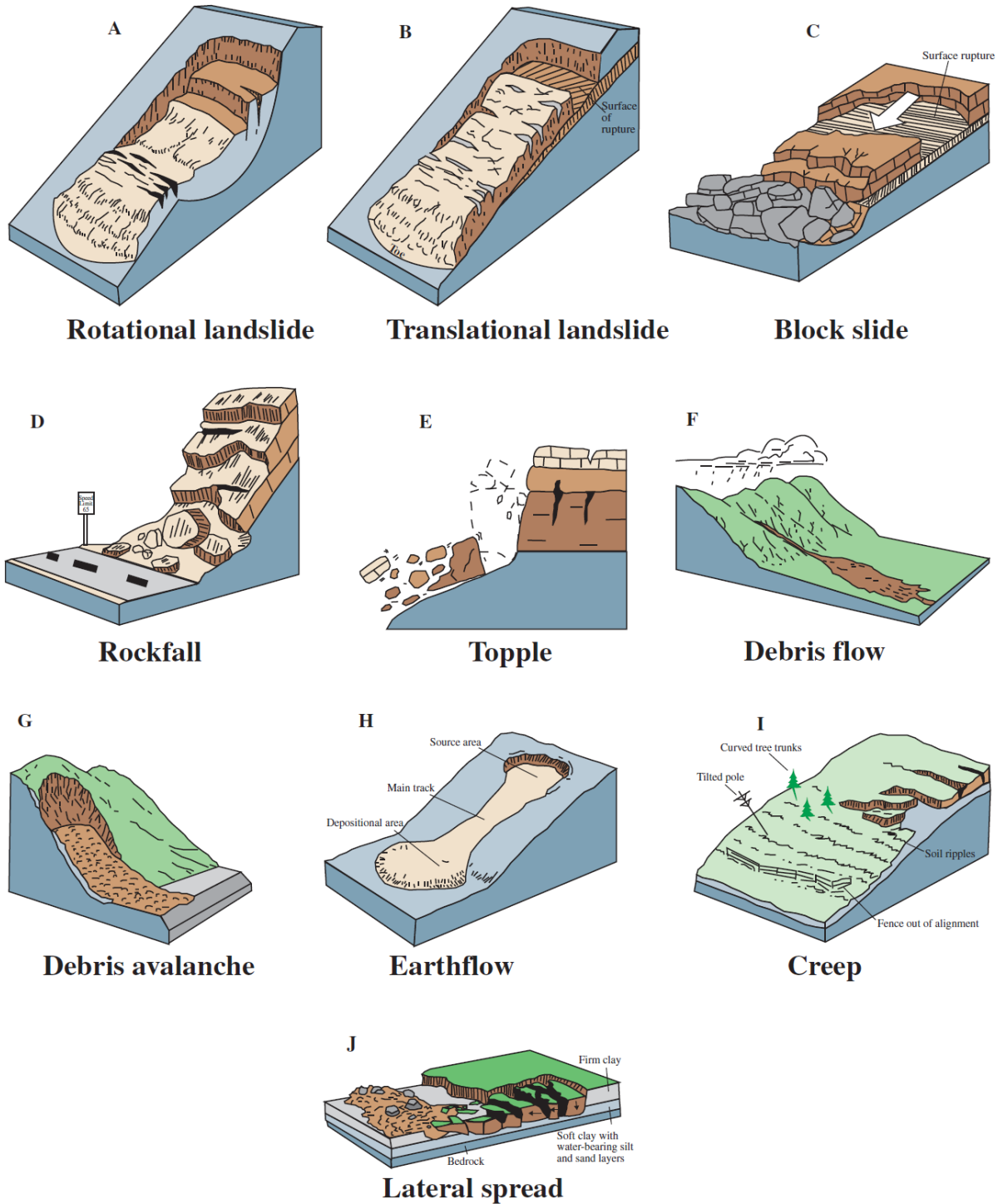


Fig. 20: Major types of landslides (USGS 2004)

Type of movement	Rock	Soil
Fall	1. <i>Rock/ice</i> fall ^a	2. <i>Boulder/debris/silt</i> fall ^a
Topple	3. Rock block topple ^a	5. <i>Gravel/sand/silt</i> topple ^a
	4. Rock flexural topple	
Slide	6. Rock rotational slide	11. <i>Clay/silt</i> rotational slide
	7. Rock planar slide ^a	12. <i>Clay/silt</i> planar slide
	8. Rock wedge slide ^a	13. <i>Gravel/sand/debris</i> slide ^a
	9. Rock compound slide	14. <i>Clay/silt</i> compound slide
	10. Rock irregular slide ^a	
Spread	15. Rock slope spread	16. <i>Sand/silt</i> liquefaction spread ^a
		17. Sensitive clay spread ^a
Flow	18. <i>Rock/ice</i> avalanche ^a	19. <i>Sand/silt/debris</i> dry flow
		20. <i>Sand/silt/debris</i> flowslide ^a
		21. Sensitive clay flowslide ^a
		22. Debris flow ^a
		23. Mud flow ^a
		24. Debris flood
		25. Debris avalanche ^a
		26. Earthflow
		27. Peat flow
		Slope deformation
29. Rock slope deformation	31. Soil creep	
	32. Solifluction	

Fig. 20: Landslide classification scheme (Hungr et al. 2014)

Velocity class	Description	Velocity (mm/s)	Typical velocity	Response ^a
7	Extremely rapid	5×10^3	5 m/s	Nil
6	Very rapid	5×10^1	3 m/min	Nil
5	Rapid	5×10^{-1}	1.8 m/h	Evacuation
4	Moderate	5×10^{-3}	13 m/month	Evacuation
3	Slow	5×10^{-5}	1.6 m/year	Maintenance
2	Very slow	5×10^{-7}	16 mm/year	Maintenance
1	Extremely Slow			Nil

Fig. 22: Landslide velocity scales (Hungr et al. 2014)

Material name	Character descriptors (if important)	Simplified field description for the purposes of classification	Corresponding unified soil classes	Laboratory indices (if available)
Rock	Strong	Strong—broken with a hammer		UCS>25 MPa
	Weak	Weak—peeled with a knife		2<UCS<25 MPa
Clay	Stiff	Plastic, can be molded into standard thread when moist, has dry strength	GC, SC, CL, MH, CH, OL, and OH	$I_p > 0.05$
	Soft			
	Sensitive			
Mud	Liquid	Plastic, unsorted remolded, and close to Liquid Limit	CL, CH, and CM	$I_p > 0.05$ and $I_L > 0.5$
Silt, sand, gravel, and boulders	Dry	Nonplastic (or very low plasticity), granular, sorted. Silt particles cannot be seen by eye	ML	$I_p < 0.05$
	Saturated		SW, SP, and SM	
	Partly saturated		GW, GP, and GM	
Debris	Dry	Low plasticity, unsorted and mixed	SW-GW	$I_p < 0.05$
	Saturated		SM-GM	
	Partly saturated		CL, CH, and CM	
Peat		Organic		
Ice		Glacier		

Fig. 23. Landslide forming material (Hungri et al. 2014)

Figs 18 to 23 show classification schemes for mass flow phenomena. Figs 24 and 25 show a rockfall in a sandstone massive (Wartturm) in the Elbe valley south of Dresden (Germany). Fig. 26 shows a corresponding simple numerical model, which illustrates the failure pattern: tensile crack originated from a fracture with weathering traces (brown area in Fig. 25). Calibration of the model using lab tests has allowed to predict this rockfall. Fig. 27 shows a foto of a sandstone massive nearby and the corresponding 3-dimensional model. As explained in detail by Herbst & Konietzky (2012) the factor-of-safety can be determined by considering different techniques (e.g. $c-\phi-\sigma_t$ -reduction) and considering different processes (e.g frost-thaw changes or specific weathering). Also, potential rock fall locations can be predicted.

Quite common are so-called 'rockfall simulation programs'. They consider the rockfall process by calculating the sliding and jumping of particles under consideration of the slope profile, vegetation, fences etc. A stochastic analysis allows run-out prediction and dimensioning of rockfall fences or other barriers. Fig. 28 shows the application of such a tool in a 2-dimensional version.



Fig. 24: Rockfall in a sandstone massive (Germany): (a) before rockfall, (b) after rockfall, (c) detailed view of rockfall

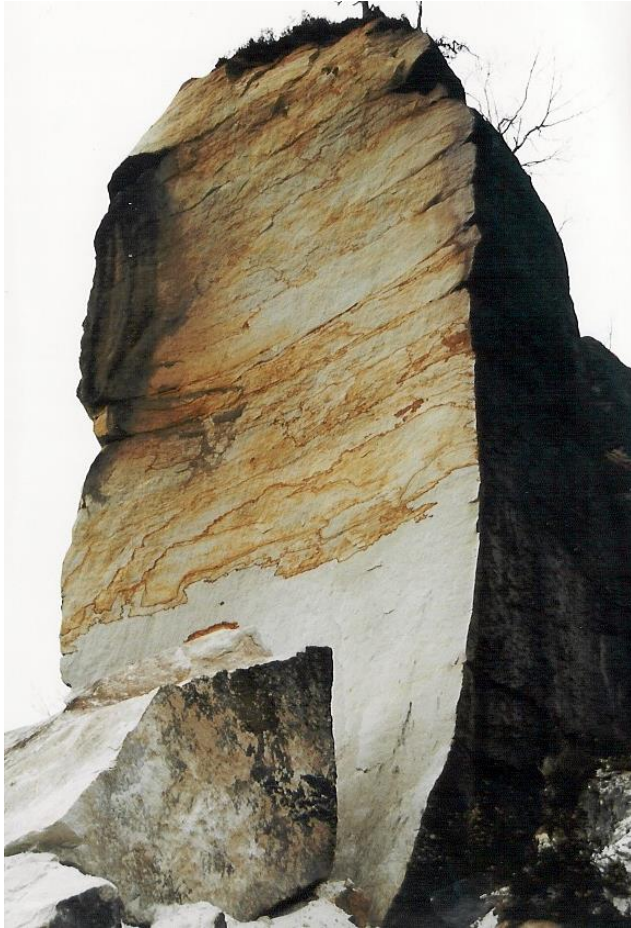


Fig. 25: Weathering (red-brown colored rock surface) indicates the existence of a fracture; white colored part shows fresh fracture created by rockfall (see Fig. 20)

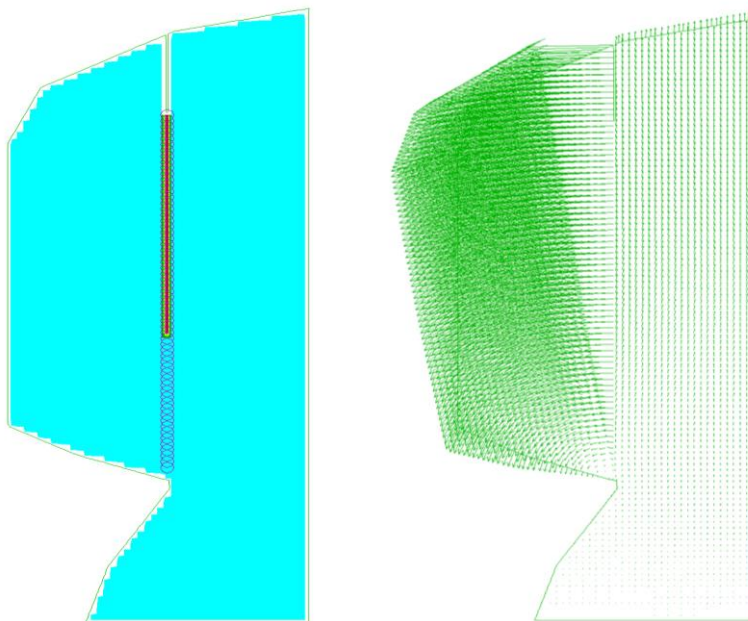


Fig. 26: Simple numerical model to backanalyze rockfall (see Figs 20 and 21)



Fig. 27: Sandstone massive (Germany) and corresponding 3D model indicating potential rockfall areas (Herbst & Konietzky, 2012)

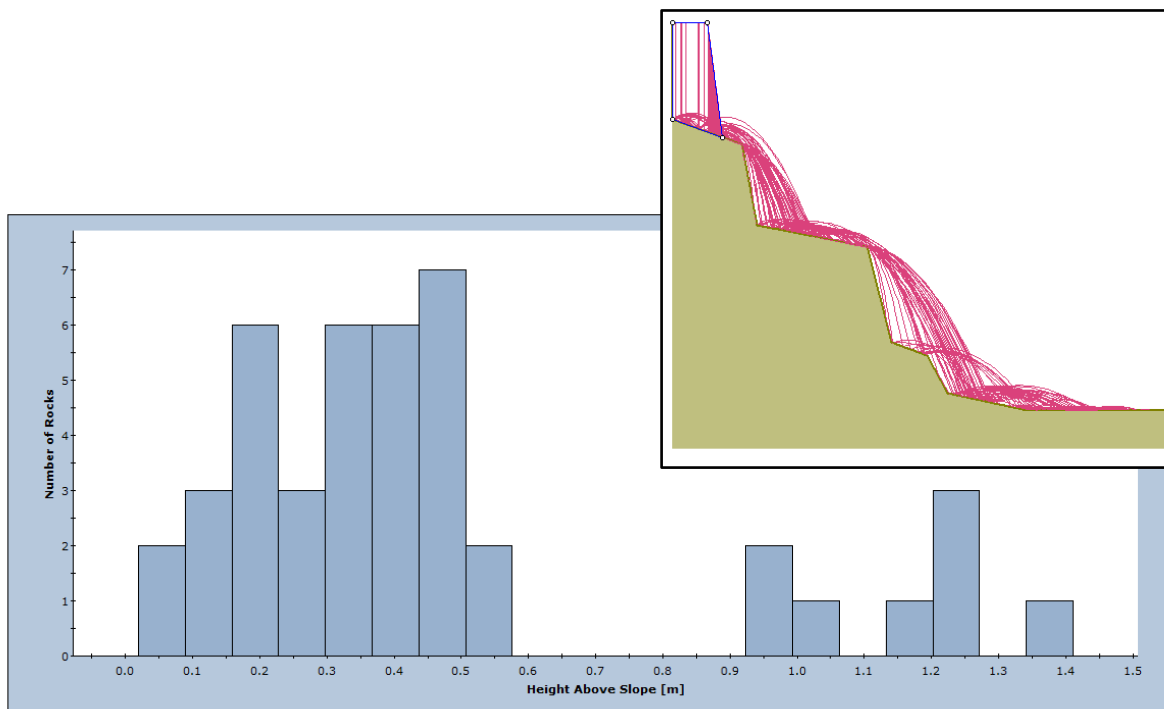


Fig. 28: Simple stochastic rockfall analysis based on 100 falling, sliding, jumping balls (paths and ball jumping height statistic for a certain position along slope)

5 Explosions

Large explosions, especially nuclear explosions, can cause tremendous damage of the earth crust. Exemplary, Tab. 1 gives some data about the Chagan nuclear explosion, exploded at a depth of nearly 200 m below the surface in a sandstone formation producing a crater of 500 m diameter moving several million cubic meter of rock mass. Besides the produced vibrations (recognizable by sesimometers all over the world) radioactive pollution of the water, soil and rock mass takes place and leads to very long-term pollution. Deep underground explosions, like the one executed at 600 m below the surface, leads to severe fracturing up to 1,000 m distance from the source. Fig. 29 shows a foto of a water filled crater produced by an undeground nuclear explosion and Fig. 30 shows numerical simulation results for near-surface and deep underground nuclear explosions.

Tab 1: Data for Chagan nuclear explosion (Semipalatinsk test area)

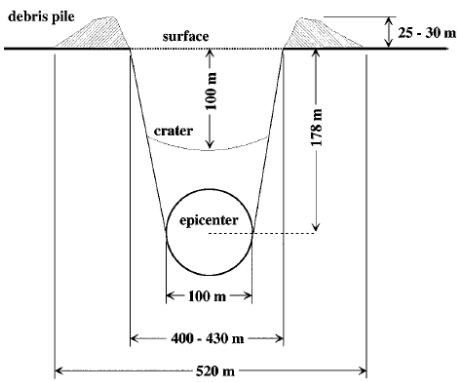
The Chagan Nuclear Test		
Date		15 January 1965
Coordinates		40°56'06.0'' latitude north 70°00'33.7'' longitude west
Rock type		Sandstone
Bomb strength		app. 140 kt
Depth of detonation		178 m
Crater		
Final depth		app. 100 m
Height of the debris piles		25-30 m
Diameter at the crest		app. 520 m
Diameter at the initial ground level		app. 400-430 m
Apparent crater		
Volume from the crest		app. $10.3 \times 10^6 \text{ m}^3$
Volume from initial ground level		app. $6.4 \times 10^6 \text{ m}^3$
True crater		
Volume from the crest		app. $17.7 \times 10^6 \text{ m}^3$
Volume from initial ground level		app. $14.0 \times 10^6 \text{ m}^3$
Debris		
Fragment movements from the epicentre		up to app. 1000 m
Debris volume		app. $6.7 \times 10^6 \text{ m}^3$



Fig. 29: Water filled crater (500 m in diameter) in the Semipalatinsk test area

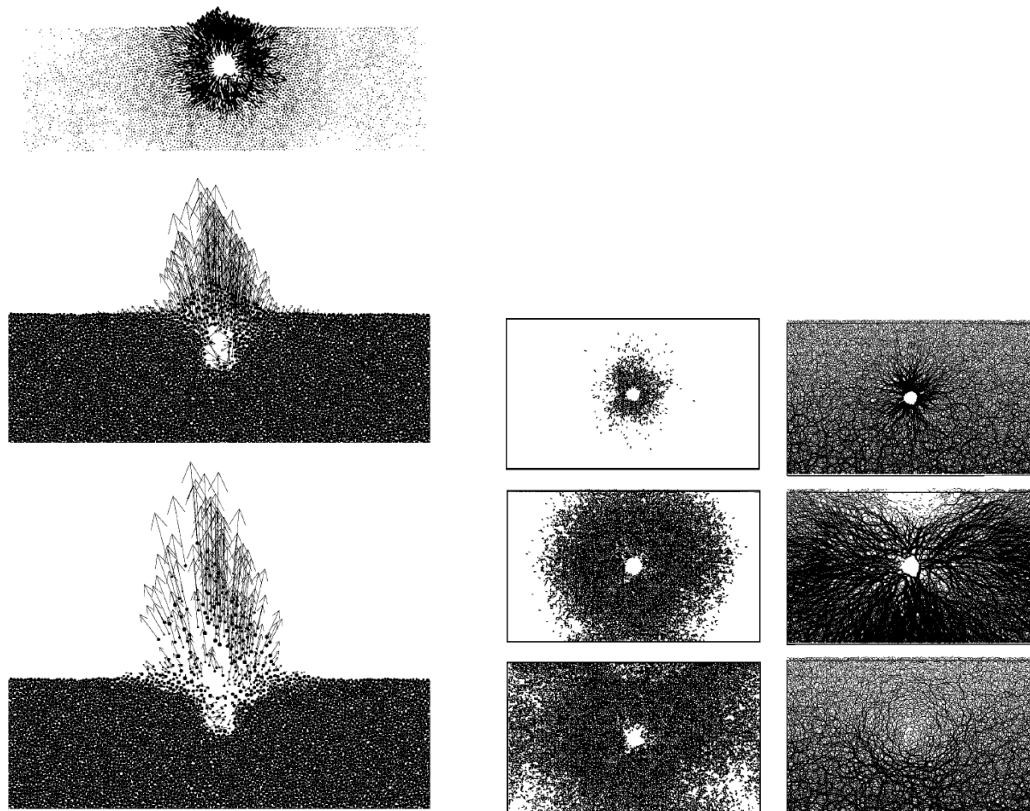


Fig. 30: Numerical models of nuclear explosions in Semipalatinsk test area: left: near-surface explosion, right: underground explosion (te Kamp et al. 1998)

6 References

- BGS (2016): <https://www.bgs.ac.uk/research/engineeringGeology>
- Bommer, J. et al. (2006): Control of hazard due to seismicity induced by hot fractures rock geothermal project, *Engineering Geology*, 83: 287-306
- Cruden, D.M., Varnes, D.J. (1996): Landslide Types and Processes, Special Report, Transportation Research Board, National Academy of Science, 247: 36-75
- DIN4150-3 (1999). Erschütterungen im Bauwesen, Einwirkungen auf bauliche Anlagen, Deutsches Institut für Normung
- Fenton, G.A.; Griffiths, D.V. (2008): Risk assessment in geotechnical engineering, John Wiley & Sons, 461 p.
- Grünthal, G. (2014): Induced seismicity related to geothermal projects versus natural tectonic earthquakes and other types of induced seismic events in Central Europe, *Geothermics*, 52: 22-35
- Herbst, M.; Konietzky, H., (2012): Numerical modelling of natural rock formations to estimate stability using the example of a sandstone massif in Saxony, *Geomechanics and Tunneling*, 4: 379-388
- Hungr, O. et al. (2014): The Varnes classification of landslide types - an update, *Landslides*, 11: 167-194
- Leine, R.I. et al. (2014): Simulation of rockfall trajectories with consideration of rock shape, *Multibody Syst Dyn*, 32: 241-271
- Ma, G. et al. (2011): Practical studies on rockfall simulation by DDA, *J. Rock Mech. Geotechn. Eng.*, 1: 57-63
- Poisel, R.; Preh, A. (2004): Rock Slope Initial Failure Mechanisms and their Mechanical Models, *Felsbau*, 22: 40–45
- Schütz, H.; Konietzky, H. (2016): Evaluation of flooding induced seismicity from the mining area Schlema/Alberoda (Germany), *Rock Mechanics Rock Engineering*, 49: 4125-4135
- Siskind, D.; Stagg, M.; Kopp, J.; Dowding, D. (1980): Structure response and damage produced by ground vibration from surface mine blasting. Report RI8507, United States Bureau of Mines.
- te Kamp, L.; Konietzky, H.; Guerin F. (1998): Modelling of the Chagan underground nuclear test with the distinct element method, *FRAGBLAST*, 2: 295-312
- USGS (2004): Landslide types and processes, U.S. Geological Survey, Fact Sheet 2004-3072